Applied Energy 269 (2020) 114954

Contents lists available at ScienceDirect

Applied Energy

journal homepage: www.elsevier.com/locate/apenergy

Advanced power cycles for coal-fired power plants based on calcium looping combustion: A techno-economic feasibility assessment

Sebastian Michalski, Dawid P. Hanak*, Vasilije Manovic

Energy and Power, School of Water, Energy and Environment, Cranfield University, Bedford, Bedfordshire MK43 0AL, UK

HIGHLIGHTS

- Carbonate looping can reduce economic and efficiency penalties of carbon capture.
- Advanced power cycles can improve the performance of power generation systems.
- Recompression supercritical CO_2 cycle led to the best techno-economic performance.
- Efficiency (38.9%) was higher than that of reference coal-fired power plant (38.0%).
- Cost of CO_2 avoided (16.3 €/t) was lower than the current carbon tax (> 18 €/t).

ARTICLE INFO

Keywords:
Efficiency penalty
Carbon capture
Clean power technologies
Clean coal
Carbonate looping
Advanced power generation

ABSTRACT

Carbon capture and storage is crucial to decarbonising the power sector, as no other technology can significantly reduce emissions from fossil fuel power generation systems. Yet, the mature CO_2 capture technologies result in net efficiency penalties of at least 7% points. Emerging technologies, such as calcium looping combustion, can reduce the net efficiency penalty to 2.4% points. Further reductions can be achieved by replacing the conventional steam cycle with advanced power cycles. This study aimed to assess the techno-economic feasibility of the coal-fired power plant based on calcium looping combustion with different advanced Brayton cycles. These included single power cycles, such as recompression supercritical CO_2, simple supercritical CO_2 cycle, and xenon cycle, as well as combined power cycles based on helium, nitrogen and recompression supercritical CO_2 cycles. The net efficiency and break-even electricity price, which was estimated using the net present value method, were used as the key techno-economic performance indicators. A parametric study was also conducted to assess the impact of the key thermodynamic parameters. This study showed that the case based on a single recompression supercritical CO_2 cycle had the best overall techno-economic performance, while the recompression supercritical CO_2 combined cycle case had the best techno-economic performance among combined cycle cases. The former was characterised with a net efficiency of 38.9%, which is higher than that of the reference coal-fired power plant without CO_2 capture (38.0%). Such performance was achieved at a break-even electricity price of 71.2 €/$MW_{el,net}$h, corresponding to a cost of CO_2 avoided of 16.3 €/t_{CO2}.

1. Introduction

Meeting the ambitious emission reduction targets established in the Paris Agreement requires near-complete decarbonisation of the power sector [1], as this sector generates a third of the anthropogenic greenhouse gas emissions [2]. Despite the potential improvements in their efficiency, conventional fossil-fuel-fired power plants are not able to meet the environmental targets. As no other technologies can significantly reduce emissions from fossil fuel power generation systems, which are predicted to play an important part in the future electricity portfolio, carbon capture and storage (CCS) is seen as crucial to decarbonising the power sector [3].

Regardless of significant reductions in the energy intensity of mature CO_2 capture and separation technologies [4], integration of CCS to fossil-fuel-fired power plants is still expected to reduce the net efficiency of the

Abbreviations: CaL, carbonate looping; CaLC, calcium looping combustion; CBC, closed Brayton cycle; CCS, carbon capture and storage; CCT, CO_2 compression train; CGC, clean gas cooler; COM, compressor; EXP, expander; FGC, flue gas cooler; CON, condenser; HHV, higher heating value; MEA, monoethanolamine; NPV, net present value; REC, recompressor; ReS, refrigeration system; RHX, recuperator; sCO_2, supercritical CO_2 cycle

* Corresponding author.
E-mail address: d.p.hanak@cranfield.ac.uk (D.P. Hanak).

https://doi.org/10.1016/j.apenergy.2020.114954
Received 23 April 2019; Received in revised form 1 April 2020; Accepted 2 April 2020
0306-2619/ © 2020 The Authors. Published by Elsevier Ltd. This is an open access article under the CC BY license (http://creativecommons.org/licenses/BY/4.0/).

Nomenclature

$\dot{m}_F$	fuel flow rate
BEP_{el}	break-even price of electricity
C_{CaLC}	investment costs of CaLC
C_{CCT}	investment costs of CCT
C_{cycle}	investment costs of power cycle
CF_t	annual cash flow
C_{Inv}	investment cost
$C_{L\&O}$	land and owner's cost
$i_{E\&PC}$	engineering and project cost indicator
i_{LC}	labour cost indicator
$i_{P\&C}$	integration costs indicator
i_{TASC}	total as-spent cost (TASC) multiplier
HHV	higher heating value
NPV	net present value
r	discount rate
$\sum P_{AUX}$	total auxiliary power requirement
η_N	net efficiency of power plant
$\eta_{indirect}$	efficiency of indirect heat transfer

entire system by at least 7.2% points [5] while using solutions of piperazine (PZ) instead of monoethanolamine (MEA). Importantly, reduction in the net efficiency and the capital cost associated with CCS have been shown to lead to at least 60% increase in the electricity cost [6]. Therefore, to provide incentives for CCS deployment in the power sector, less energy-intensive technologies, such as solid looping cycles, are currently being developed. Carbonate looping (CaL), which is based on the reversible carbonation reaction of CO_2 with a metal oxide, such as calcium oxide, is regarded as an emerging technology for decarbonisation of fossil-fuel-fired power generation systems [7]. This is because it has the potential to reduce the net efficiency penalties to 5% points [8]. The main reason behind such an improvement, when compared to the mature CO_2 capture and separation technologies, is the high-temperature operation of CaL (600–900 °C). This enables utilisation of high-grade heat for power generation in a secondary power cycle. Importantly, the net power output of the retrofitted system has been shown to increase by 40–60% after utilisation of the high-grade heat in a conventional steam cycle, compared to the conventional fossil-fuel-fired power plant without CCS [9].

To achieve a further reduction in the energy intensity of CaL, which is mainly associated with the power requirement of the air separation unit, indirect heat transfer from an external heat source to drive the sorbent regeneration process can be deployed. Indirectly-heated fluidised bed dryers, calciners, and mixing devices have been proposed in the 1980s by Rossi [10] and reviewed by Malhotra and Mujumdar [11]. Indirectly-heated calciners were considered for several industrial applications, including production of phosphoric acid waste gypsum [12], and pyrolysis and gasification of solid fuels [13]. More recently, indirectly-heated calciners were also tested experimentally [14] and considered as a basis for process development [15] for energy storage from concentrating solar plants. Application of indirectly-heated calciners to calcium looping was first proposed by Abanades et al. [16] and its technical feasibility was later proven by Junk et al. [17] and Hoeftberger and Karl [18].

Due to the high-temperature operation of CaL, it can act as the primary heat source in low-CO_2-emission fossil-fuel-fired power generation systems. Therefore, Hanak and Manovic [19] proposed the concept of calcium looping combustion (CaLC) that integrates an air-fired combustor with a calciner to drive the calcination process. When linked with a conventional supercritical steam cycle, coal-fired power plants based on CaLC achieved net efficiencies as high as 35.6% [19]. This was 2.4% points below the conventional coal-fired power plant with the steam cycle operating under the same steam conditions. Recent trends in the development of nuclear and solar power generation systems, which operate within the temperature envelope of 500–1000 °C, indicated that advanced power cycles can increase the net efficiency and decrease the investment costs of the entire system, compared to those equipped with the conventional steam cycle [20].

A supercritical CO_2 (sCO_2) cycle has been recently considered as a feasible alternative to the conventional steam cycle in concentrating solar plants [21], coal-fired power plants [22], natural gas combined cycle power plants [23] and natural gas-fired power plants based on chemical looping combustion [24]. Furthermore, the work by Hanak and Manovic [7] has revealed that replacing the supercritical steam cycle with the recompression sCO_2 cycle to utilise the high-grade heat available in CaL can increase the net efficiency of the entire system by 1.0–2.2% points, depending on the structure and operating conditions of the power cycle. On the contrary, Michalski et al. [25] has shown that the net efficiency of CaLC with simple sCO_2 cycle is 0.9% points lower than that of CaLC with steam cycle. This implies that only the recompression sCO_2 cycle has the potential to achieve the desired efficiency improvement. It also needs to be highlighted that, regardless of the higher net efficiency than for the CCS retrofits, the coal-fired power plant based on CaLC was shown to be characterised with 37% higher break-even cost of electricity than that of the coal-fired power plant without CCS (59.63 €/$MW_{el,net}$h) [25]. Such an increase was shown to be lower than that for an amine scrubbing retrofit (62%) and CaL retrofit (44%).

Further improvement in the techno-economic feasibility of the coal-fired power plant based on CaLC can be achieved through revision of the sCO_2 cycle structure and operating conditions, as well as consideration of other advanced power cycles, such as closed Brayton cycles (CBC) using different working media. These power cycles are currently at a lower maturity level than the conventional steam cycle. Yet, sCO_2, helium (He) and nitrogen (N_2) CBCs are commonly considered power cycles for nuclear power plants [26]. Importantly, the CBC based on N_2 has been considered as a near-term demonstration concept [27], as the deployment of the sCO_2 cycle still depends on substantial technological developments in turbomachinery [28] and heat exchangers [26] and the He cycle is not competitive from the thermodynamic standpoint [29]. Xenon (Xe) has also been shown as a potential CBC working medium that enables achieving high efficiencies [30]. Although application of these advanced power cycles has been evaluated for nuclear power plants and solar power plants, their application to coal-fired power plants has not been considered, with the exception of the sCO_2 cycle.

Therefore, this study proposes to integrate the advanced power cycles with CaLC for high-efficiency power generation with low CO_2 emissions and affordable cost of electricity. To assess the techno-economic feasibility of the proposed designs of the coal-fired power plant based on CaLC, process models for each advanced power cycle were developed in Aspen Plus® and validated with the data available in the literature, before integration with CaLC. The techno-economic performance was assessed considering the net efficiency and the break-even price of electricity (BEP_{el}). Furthermore, as the current literature provides limited information on the operating conditions of the advanced power cycles considered in this study, a parametric study on the key design parameters, such as the compressor outlet pressure, turbine inlet temperature and minimum temperature differences, was carried out to maximise the techno-economic performance of the considered cases. Finally, to account for the uncertainty in market conditions, the effect of carbon tax on the economic performance was evaluated.

2. Process description

The layout of each coal-fired power plant based on CaLC evaluated in this work can be divided into three main subsystems: CaLC; CO_2 compression train (CCT); and power cycle. The structure of the CaLC (Fig. 1) has been described in detail by Hanak and Manovic [19]. It

comprises two interconnected fluidised beds: a carbonator, where CO_2 from flue gas is removed by CaO at 650 °C; and a calciner where $CaCO_3$ is regenerated to CaO at 900 °C achieved by indirect heat transfer from the combustor to the calciner via a heat transfer wall [16]. The process model for CaLC has been developed in Aspen Plus® based on the CaL model developed by Hanak et al. [8] and validated using experimental data from the la Pereda pilot plant (Spain) [31]. To account for sorbent deactivation and its effect on the techno-economic performance, the maximum average conversion was represented using the semi-empirical model proposed by Rodríguez et al. [32] and Li et al. [33] The deactivation curve was taken from the la Pereda pilot plant results [31]. The combustor is assumed to be a circulating fluidised bed that operates at atmospheric pressure and 1000 °C, and is fuelled with coal with a higher heating value (HHV) of 27.01 MJ/kg [25]. The high-grade heat from the flue gas cooler (FGC), carbonator and clean gas cooler (CGC) is utilised for power generation. It is assumed that the minimum temperature difference of the CGC is 20 °C. Finally, the CO_2 capture rate in the carbonator is adjusted to achieve an overall CO_2 capture level of 90% [34] considering both CO_2 produced from fuel combustion and calcination of fresh sorbent. The heat losses in the reactors are not considered. The remaining assumptions regarding the operating conditions of CaLC are presented in Table 1.

The concentrated CO_2 stream from the calciner is subsequently fed into the CCT (Fig. 1). This subsystem is equipped with a nine-stage intercooled compressor, which is characterised with a polytropic efficiency of 77–80%, CO_2 condenser (CON) and CO_2 pump that has an isentropic efficiency of 85%. The mechanical efficiency of the CO_2 pump and compressor is 99.6%. The intercooler's outlet temperature is 40 °C and the overall heat transfer coefficient is 300 W/m^2°C. The CCT compresses the CO_2 stream to 11 MPa.

2.1. Recompression supercritical CO_2 cycle (sCO_2 RC2E2 case)

The structure of the recompression sCO_2 cycle, which uses CO_2 in a supercritical state as a working medium, integrated with CaLC (sCO_2 RC2E2 case) is presented in Fig. 1. The thermodynamic model of this advanced power cycle was based on the recompression sCO_2 cycle model developed in Aspen Plus® by Hanak and Manovic [7]. This model has been validated with the thermodynamic results presented by Le Moullec [35] and experimental results presented by Park et al. [36]. The validation results are presented in the Supplementary Information. The highest difference in comparison with modelling data is for the compressor outlet temperature (1.85%), while for the experimental data the highest difference is for the expander outlet temperature (2.24%). For the remaining parameters, the relative error is below 0.5%. In this study, the structure of the recompression sCO_2 cycle has been adapted by adding a CGC that enabled reducing the temperature of clean gas to temperature levels of the flue gas at the outlet of the air preheaters in conventional coal-fired power plants (85–125 °C) [37]. Additionally, a two-stage expander and a two-stage intercooled compressor were considered.

In the considered sCO_2 cycle, a two-stage expander (EXP1 and EXP2) with isentropic efficiency of 93% is used. After expansion, the CO_2 stream is cooled down in two recuperators (RHX1 and RHX2). Then, the CO_2 stream is split into two streams feeding the recompressor (REC) with an isentropic efficiency of 85% and cooler, where it is cooled down to 31.3 °C. The cooled CO_2 stream is then compressed from 7.4 MPa to 20 MPa in a two-stage intercooled CO_2 compressor (COM1 and COM2) with an isentropic efficiency of 85%. Then, the CO_2 stream leaving COM2 is split into two streams feeding the low-temperature CGC2 and RHX2. For the RHX2, a cold-end temperature

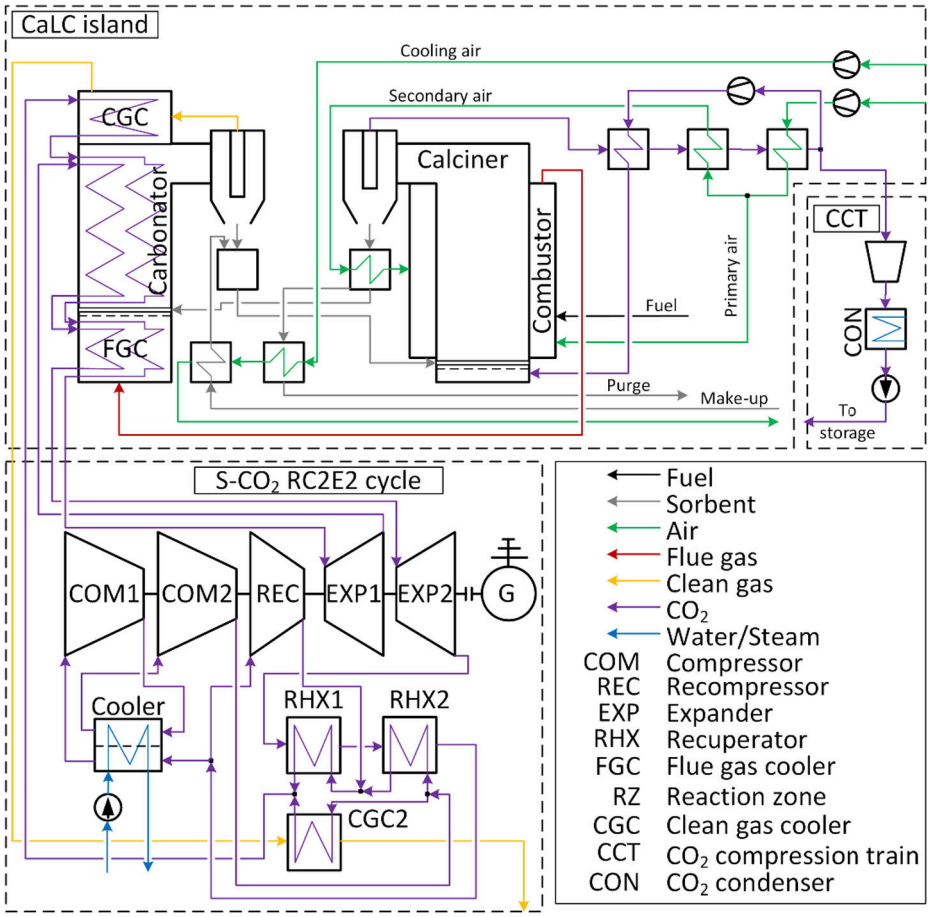


Fig. 1. A process flow diagram of calcium looping combustion with recompression supercritical CO_2 cycle (sCO_2 RC2E2 case).

Table 1
Initial process model assumptions for calcium looping combustion [19].

Subsystem	Parameter	Value
Combustor	Flue gas outlet temperature (°C)	1000
	Pressure drop (kPa)	15
Calciner	Operating temperature (°C)	900
	Pressure drop (kPa)	15
	Calcination extent (–)	0.95
	Recycled CO_2 fraction (–)	0.2
Carbonator	Operating temperature (°C)	650
	Pressure drop (kPa)	15
	Carbonation extent (–)	0.7
Heat exchanger network	Sorbent cooler and heater minimum temperature approach (°C)	25.0
	Air preheater minimum temperature approach (°C)	10.0
	CO_2 preheater minimum temperature approach (°C)	10.0
	Cold-/hot-end temperature difference in the compressor intercooler (°C)	15/30
	Cold-/hot-end temperature difference in the last captured CO_2 cooler (°C)	5/30
Auxiliary power assumptions	Coal handling system specific power consumption (MJ/t_{coal})	8.2
	Sorbent handling system specific power consumption ($MJ/t_{sorbent}$)	52.4
	Ash and used sorbent handling system specific power consumption ($MJ/t_{ash/sorbent}$)	31.2

difference of 5 °C was assumed. The CO_2 stream is then mixed with the stream from REC and then fed into RHX1, where a cold-end temperature difference of 10 °C was assumed. Then, hot CO_2 streams from RHX1 and CGC2 are mixed and further heated to 600 °C, utilising the high-grade heat available in the CGC, carbonator and FGC. The CO_2 stream is then fed into the first stage of the expander. The CO_2 stream is reheated in the carbonator and FGC to 600 °C and fed into a second stage of the expander.

The split ratios of the CO_2 stream before the cooler and at the outlet of COM2 are adjusted to achieve a RHX2 hot-end temperature difference of 5 °C and the same temperature of the CO_2 streams leaving RHX1 and CGC2. Heat transfer coefficient of 1700 W/m^2 °C and 2900 W/m^2 °C for RHX and cooler were assumed, respectively [20]. Other assumptions and design specifications for the sCO_2 cycle are presented in Table 2.

2.2. Xenon cycle (Xe case) and simple sCO_2 cycle (sCO_2 PE2 case)

The structure of the Xe cycle integrated with CaLC (Xe case) is presented in Fig. 2. The thermodynamic model of the Xe cycle was developed in Aspen Plus® and validated based on data presented by Garcia [30]. The validation results are presented in the Supplementary Information and showed that the temperature at the outlet of the pump was overestimated by 1.2 °C (1.35%), with the remaining temperatures varying only by up to 0.15 °C. The same structure of power cycle (Fig. 2) is also used for the sCO_2 cycle (sCO_2 PE2 cycle).

In the considered advanced cycle, the supercritical pump (SCP) with an isentropic efficiency of 85% was used instead of the intercooled compressor and recompressor in the recompression sCO_2 cycle (RC2E2). It was assumed that the pressure at the inlet to the pump is 4.85 MPa and 7.3 MPa for Xe and sCO_2 cycle, respectively. Those pressures correspond to the saturation temperature of 7.5 °C for Xe and of 31 °C for CO_2. As a result, a refrigeration system (ReS), which has the coefficient of performance (COP) of 6.4 [38], needed to be added into the Xe cycle. Moreover, the Xe stream temperature of 27 °C at the outlet of the cooler and the relative pressure loss in ReS of 1% were assumed. The pump increases the pressure to 30 MPa. An isentropic efficiency of 93% was assumed for the expanders [39]. Additionally, the advanced power cycle contains only one recuperator (RHX1), for which a cold-end temperature difference of 5 °C was assumed [35]. The split ratio of the working fluid stream at the outlet of the SCP is adjusted to achieve the same temperature as the streams leaving RHX1 and CGC2.

The overall heat transfer coefficients for the RHX1 and cooler in the Xe cycle of 605 $W/m^{2\circ}C$ and 1052 $W/m^{2\circ}C$ were assumed, respectively. Those coefficients were estimated using the heat transfer model [40]. The remaining assumptions are the same as in the recompression sCO_2 cycle described in Section 2.2 and presented in Table 2.

2.3. Helium combined cycle (He case)

The structure of a He combined cycle integrated with CaLC (He case) is presented in Fig. 3. The thermodynamic model of a topping He cycle was developed in Aspen Plus® and benchmarked with the model developed by Kunitomi et al. [41]. The validation results are presented in the Supplementary Information. It needs to be highlighted that in contrast to the sCO_2 RC2E2 cycle, the He cycle has one recuperator instead of two and there is no recompressor. Another important difference is that there is no heat exchanger parallel to the recuperator (RHX1). This is because, at the assumed temperature difference of 5 °C at the RHX1 cold end, the temperature difference at the hot end of RHX1 is 5.3 °C.

In the considered topping He cycle, an intercooled compressor with a polytropic efficiency of 90.5% increases the He stream pressure from 3.5 MPa to 9 MPa. The expander isentropic efficiency of 92.8% and the temperature of 27 °C of the He stream at the outlet of the cooler were assumed. Importantly, the preliminary results showed that the outlet temperature of clean gas was still high (> 480 °C) and would lead to substantial heat loss, affecting the overall efficiency of the entire system. Therefore, a bottoming He cycle was implemented to utilise the high-grade heat available in the clean gas stream. This cycle comprises a single-stage expander, as opposed to the two-stage expander in the topping He cycle. Moreover, the same pressures and pressure loss coefficients were assumed in both the topping and bottoming He cycles. The live temperature of He in the bottoming cycle was a result of the assumed minimum temperature difference of 20 °C in CGC2. Finally, the overall heat transfer coefficients of 750 $W/m^{2\circ}C$ and 2591 $W/m^{2\circ}C$ were assumed for the RHX and cooler, respectively. Those coefficients are based on the heat transfer model [40,42,43]. The remaining assumptions are the same as those presented in Table 2.

Table 2
Process model assumptions for advanced power cycles.

Parameter	Value
Relative pressure loss in cold side of RHX heat exchanger (%)	0.5
Relative pressure loss in hot side of RHX heat exchanger (%)	1.0
Relative pressure loss in cold side of CGC heat exchangers (%)	0.3
Relative pressure loss in cold side of carbonator heat exchanger (%)	0.5
Relative pressure loss in cold side of FGC heat exchangers (%)	0.2
Relative pressure loss in hot side of cooler (%)	1.0
Live and reheated temperature of working medium (°C)	600
Electric generator efficiency (%)	98.5
Mechanical efficiency (%)	99.0
Cooling water parameters at the inlet to the water pump (°C/MPa)	20/0.1
Water pump pressure ratio (–)	2.0
Water temperature at the outlet of cycle medium cooler (°C)	25

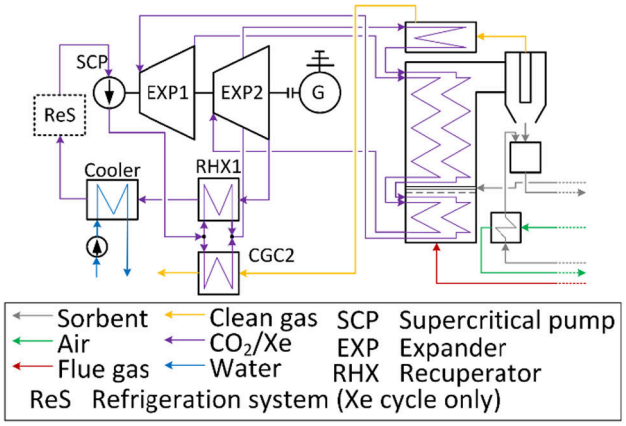


Fig. 2. A process flow diagram of carbonator integrated with Xe cycle and simple supercritical CO_2 cycle (sCO_2 PE2 cycle).

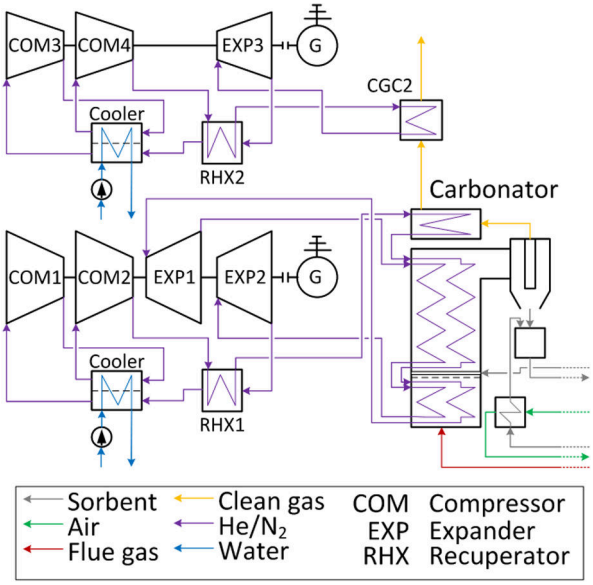


Fig. 3. A process flow diagram of carbonator integrated with He combined cycle (He case) and N_2 combined cycle (N_2 case).

2.4. Nitrogen combined cycle (N_2 case)

The structure of N_2 combined cycle integrated with CaLC (N_2 Case) is the same as for the He combined cycle (Fig. 3). The thermodynamic model of the main N_2 cycle was developed in Aspen Plus® based on the data provided and benchmarked against the results reported by Olumayegun et al. [26]. The validation results are presented in the Supplementary Information.

In the considered topping N_2 cycle, the intercooled compressor with an isentropic efficiency of 88% increases the N_2 stream pressure from 9 MPa to 20 MPa. The expander isentropic efficiency of 90%, the temperature of N_2 at the outlet of cooler of 27 °C and the RHX cold-end temperature difference of 5 °C were assumed. Similarly to the He case, if only a topping N_2 cycle was considered, the clean gas would leave the system at around 400 °C. Therefore, a bottoming N_2 cycle was considered, with the assumption that the pressures and pressure loss coefficients are the same in the bottoming and topping cycles. The live temperature of N_2 in the bottoming cycle was a result of assumed minimal temperature difference of 20 °C in CGC2. Moreover, the overall heat transfer coefficients of 1267 W/m^2°C and 1731 W/m^2°C were assumed for the RHX and cooler, respectively. Those coefficients are based on the heat transfer model [40]. The remaining assumptions are the same as in Table 2.

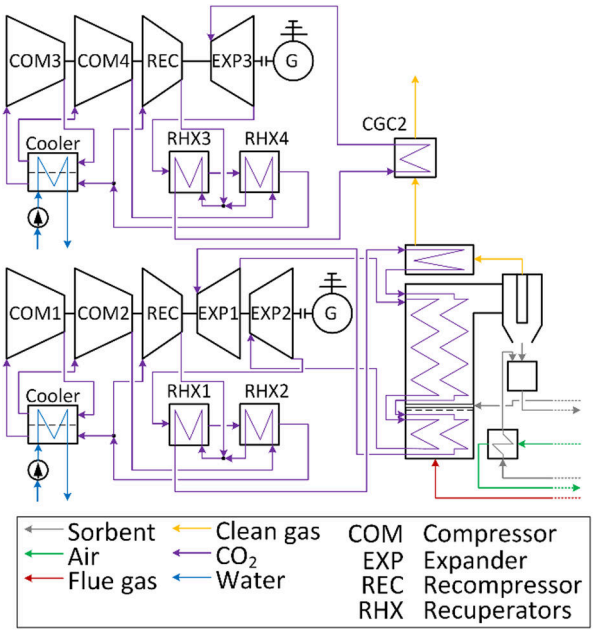


Fig. 4. A process flow diagram of carbonator integrated with supercritical CO_2 combined cycle (sCO_2 RC2E2/RC2E case).

2.5. sCO_2 combined cycle (sCO_2 RC2E2/RC2E case)

The structure of the sCO_2 combined cycle is a combination of the structure of the sCO_2 recompression cycle (Fig. 1) and He/N_2 combined cycles (Fig. 3). Thus, the recompressor was added and two recuperators (RHX1 and RHX2) were considered in the structures presented in Fig. 3. The final structure of the sCO_2 combined cycle is presented in Fig. 4. The process model assumptions for both the topping and the bottoming sCO_2 cycles were the same as presented in Section 2.1. The live temperature of CO_2 in the bottoming cycle is a result of assumed minimal temperature difference of 20 °C in CGC2 heat exchanger.

3. Techno-economic assessment methodology

The techno-economic feasibility of the cases identified in Section 2 has been assessed using the process models developed in Aspen Plus® and the methodology developed by Michalski, Hanak and Manovic [25]. This study considered the net efficiency of the entire system (η_N), which is defined in Eq. (1) as the main thermodynamic performance indicator. It depends on the gross power output (P_G), total auxiliary power requirement (ΣP_{AUX}), fuel flow rate (m_F), and higher heating value (HHV) of fuel.

$$\eta_N = \frac{P_G - \sum P_{AUX}}{\dot{m}_F \cdot HHV} \quad (1)$$

In CaLC, the auxiliary power requirement arises from the power requirements of the coal, sorbent, ash, and spent sorbent handling systems, coal pulveriser, primary air fan, cooling air fan, and CO_2 recirculation fan. The power of the CO_2 compressor and CO_2 pump make up the auxiliary power of the CCT. In the advanced power cycles, the auxiliary power consists of the power requirement of the cooling water pump, cooling tower fan, and appearing only in the Xe cycle, the power of ReS. Moreover, the ratio of heat transferred to the calciner (Q_{calc}) and the chemical energy of fuel is estimated using Eq. (2) to assess the efficiency of indirect heat transfer ($\eta_{indirect}$) from the combustor to the calciner.

$$\eta_{indirect} = \frac{\dot{Q}_{cal}}{\dot{m}_F \cdot HHV} \quad (2)$$

This study considered the break-even price of electricity (BEP_{el}) as the main economic performance indicator. The initial carbon tax value of 0 €/t_{CO2} was assumed and a parametric study of the parameter on the economic performance was conducted. To estimate the BEP_{el}, the net present value (NPV) approach, which is defined in Eq. (3) as the sum of the discounted annual cash flows (CF_t) throughout the system lifetime associated with investment, was employed. Thus, it depends additionally on the current building/operation year (t), discount rate (r), and total number of building and operation years (n). The remaining assumptions used in the economic performance assessment are presented in Table 3.

$$NPV = \sum_{t=1}^{t=n} \frac{CF_t}{(1+r)^t} \quad (3)$$

The investment costs of CaLC, CCT and corresponding advanced power cycle were estimated using the bottom-up approach, based on the component capital cost, considering the piping and integration costs indicator ($i_{P\&C}$) of 5%. Then, the total as-spent investment cost ($TASC$) was determined considering the labour cost indicator (i_{LC}), engineering and project cost indicator ($i_{E\&PC}$), TASC multiplier (i_{TASC}), land and owner's cost ($C_{L\&O}$), as well as investment costs of CaLC (C_{CaLC}), power cycle (C_{Cycle}), and CCT (C_{CCT}). The correlations used to estimate the capital cost of each piece of equipment in the coal-fired power plant based on CaLC, except for the SCP, were developed by Michalski, Hanak and Manovic [25] and are presented in Table 4. The correlation used to estimate the capital cost of the SCP (C_{CP}) has been derived considering both the pump efficiency dependence from the correlation for other pumps (C_P) and pressure ratio dependence from the correlation for compressors (C_C). Having determined the final form of the equation, the exponent and unit price of the pump were estimated based on Fout et al. [44], as it considers information for pumps with similar pressure ratios at the volumetric flow rate ranging between 3.9–18.8 m^3/s. Assuming that cycle pumps should be two times more expensive than water pumps, the SCP unit price of 31,282.8 €/(m^3/s) and exponent of 0.7 were determined.

4. Techno-economic assessment

Having assessed the thermodynamic performance of the considered cases (Table 5), the sCO_2 RC2E2/RC2E case has been shown to have the lowest total auxiliary power requirement (70.5 MW_{el}), whereas the figure associated with the Xe case was shown to be twice as high (141.7 MW_{el}). This was mainly because of the power requirement of the ReS that was necessary for the Xe cycle operation. Nevertheless, the sCO_2 PE2 case has been shown to achieve the highest net power output (510.34 $MW_{el,net}$). As the fuel consumption was kept constant across all considered cases, this case had the highest net efficiency (35.14%) and the lowest specific CO_2 emission (101.4 kg/$MW_{el,net}$h). It needs to be noted that the sCO_2 RC2E2 case was characterised with a similar net efficiency (34.97%) and specific CO_2 emissions (101.98 kg/$MW_{el,net}$h). The performance of the sCO_2 RC2E2/RC2E case was characterised with a lower net efficiency of 32.11% that could be associated with the lower temperature of the live CO_2 stream in the bottoming cycle. Importantly, despite the highest auxiliary power requirement, the net efficiency of the Xe case (31.43%) is only 0.7% points lower than that of the sCO_2 RC2E2/RC2E case, but is higher by 1.6% points and 3.4% points than that of the He case and N_2 case, respectively, showing that it could be feasible from a thermodynamic standpoint. Finally, the thermodynamic analysis revealed that the efficiency of indirect heat transfer from the combustor to the calciner is 67.52% in all considered cases. This is because neither the calciner nor the combustor is directly integrated with the power cycle. As selection of the power cycle will not affect the efficiency of indirect heat transfer, this performance indicator is not considered in the further analysis.

The results of the economic assessment showed that the lowest TASC is associated with the Xe case and the highest with the He case. The main reason for this is that the equipment cost of the He cycle is more than 1.6 times that of the Xe cycle, while the equipment cost of CaLC differs by only 9.4 M€. It should also be noted that in all cases the majority of the equipment cost is associated with CaLC (26.5–29.8%). The economic assessment of the considered cases also revealed that the sCO_2 PE2 case has the lowest BEP_{el} of 76.22 €/$MW_{el,net}$h and the sCO_2 RC2E2 case has the second lowest BEP_{el} of 78.35 €/$MW_{el,net}$h. This is because of the second highest net efficiency and second lowest specific TASC in the latter case, as well as the highest net efficiency and the lowest specific TASC in the former case. Moreover, the highest BEP_{el} of 92.23 €/$MW_{el,net}$h and 97.62 €/$MW_{el,net}$h were estimated for the He case and N_2 case, respectively. The BEP_{el} for the Xe case was higher than that of the sCO_2 PE2 by 8.3 €/$MW_{el,net}$h. Therefore, the sCO_2 PE2 case is characterised with the best techno-economic performance under the initial operating conditions.

It should be noted, however, that the TASC of the considered cases did not include the price of the working media in the advanced power cycles. Yet, the unit cost of CO_2 (1.6 $/kg), N_2 (4 $/kg), and He (52 $/kg) are significantly lower than that of the unit cost of Xe (1200 $/kg) [54,55], and can be neglected in the economic analysis. In the Xe case, however, the cost of the working medium will become a significant part of the TASC, if considered, making the Xe case not economically feasible. Therefore, only the thermodynamic analysis of the Xe case is undertaken in the latter parts of this study.

4.1. Parametric study

4.1.1. Calcium looping combustion parameters

To identify the potential for further improvements in the techno-economic performance of the considered cases, a parametric study was performed. The study by Hanak and Manovic [19] has indicated that the CaLC performance is mostly affected by the excess air, which also corresponds to O_2 content in the flue gas, and the relative sorbent make-up. Therefore, the O_2 content in the flue gas was varied between 1% and 3% [25], and the relative sorbent make-up was varied between 3% and 7% [56] in this analysis. The relative sorbent make-up is the ratio of the molar flow rates of fresh limestone added into the CaLC system and solids at the inlet to the carbonator.

The results of the thermodynamic and economic parametric studies are presented in Figs. 5 and 6, respectively. The variation in the relative

Table 3
Initial assumptions for economic analysis.

Parameter, Unit	Value
Investment characteristic	
Building time (years)	4
Investment cost distribution for first/second/third/fourth year of building period (%)	10/30/35/25
Loan repayment period (years)	15
Loan to total investment ratio (%)	80
Loan interest rate (%)	6
Income tax (%)	19
Operating and maintenance cost	
Capacity factor (%) [44]	85
Annual average salary per employee (k€) [45]	43.9
Employment rate (person/$MW_{el,gross}$) [46]	0.2
Unit cost of fresh sorbent (€/t) [44]	29.3
Unit cost of ash and of used sorbent disposal (€/t) [44]	22
Unit exploitation cost for all power cycles (€/h) [44]	403.03
Unit cost of coal (€/t) [47]	58.75
Repair cost as a fraction of total investment cost (%)	0.5–2.5
Insurance cost as a fraction of total investment cost (%)	0.2
Depreciation time (years)	10
Total as spent cost	
TASC multiplier (–) [44]	1.13
Labour cost indicator (–) [44]	0.5
Engineering and project cost indicator (–)[44]	0.35
Land and owner's cost (k€) [44]	198,940

Table 4
Summary of cost estimation methodology of individual pieces of equipment for coal-fired power plant based on calcium looping combustion.

Equipment [scaling parameter]	Correlation
Calciner [calciner heat flux, $\dot{Q}_{Cal}$ (kW)]	$C_{Cal} = 13.14 \cdot 10^6 \cdot \dot{Q}_{Cal}^{0.67}$
Carbonator [carbonator heat flux, $\dot{Q}_{Car}$ (kW)]	$C_{Car} = 16.591 \cdot 10^6 \cdot \dot{Q}_{Car}^{0.67}$
Cycle pump [volumetric flow rate of working medium, $\dot{V}_{CP}$ (m^3/s); pump inlet pressure, p_{in} (MPa); pump outlet pressure, p_{out} (MPa); pump isentropic efficiency, $\eta_{i,P}$ (–)]	$C_{CP} = 31,\ 282.8 \cdot \dot{V}_{CP}^{0.7} \cdot \frac{p_{out}}{p_{in}} \cdot ln\left(\frac{p_{out}}{p_{in}}\right) \cdot \left[1 + \left(\frac{1-0.8}{1-\eta_{i,P}}\right)^3\right]$
CO_2 compressor [equivalent mass flow rate of air, $\dot{m}_{AE,Com}$ (kg/s), compressor isentropic efficiency, $\eta_{i,Com}$ (–), compressor inlet pressure, p_{in} (MPa); equivalent air outlet pressure, $p_{AE,out}$ (MPa)] [48]	$C_C = \dot{m}_{AE,C} \cdot \frac{47.1}{1-\eta_{i,C}} \cdot \frac{p_{AE,out}}{p_{in}} \cdot ln\left(\frac{p_{AE,out}}{p_{in}}\right)$
CO_2 expander [equivalent mass flow rate of air, $\dot{m}_{AE,C}$ (kg/s), expander isentropic efficiency, $\eta_{i,E}$ (–); expander inlet pressure, p_{in} (MPa); equivalent air outlet pressure, $p_{AE,out}$ (MPa); expander inlet temperature, T_{in} (K)] [49,50]	$C_E = \dot{m}_{AE,E} \cdot \frac{392.2}{1-\eta_{i,E}} \cdot \frac{p_{in}}{p_{AE,out}} \cdot ln\left(\frac{p_{in}}{p_{AE,out}}\right) \cdot [1 + exp(0.036 \cdot T_{in} - 65.66)]$
CCT and cooling tower pumps [pump brake power P_P (kW); pump isentropic efficiency, $\eta_{i,P}$ (–)] [50]	$C_P = 3,\ 531.4 \cdot P_P^{0.71} \cdot \left[1 + \left(\frac{1-0.8}{1-\eta_{i,P}}\right)^3\right]$
Cooling tower [cooler heat flux, $\dot{Q}_{Cooler}$ (kW)] [44]	$C_{CT} = 32.3 \cdot \dot{Q}_{Cooler}$
Refrigeration system [ReS heat flux, $\dot{Q}_{ReS}$ (kW)]	$C_{HE} = 1,\ 352.3 \cdot \dot{Q}_{ReS}^{0.7}$ [€]
Electric generator [gross power output, P_G (kW)] [51]	$C_{EG} = 84.5 \cdot P_G^{0.95}$
Fuel preparation system [fuel flow rate, $\dot{m}_F$ (kg/s)]	$C_{FP} = 14,\ 158,\ 479 \cdot \dot{m}_F^{0.24}$
Fan [fan brake power, P_{Fan} (kW)] [51–53]	$C_{Fan} = 103,\ 193 \cdot \left(\frac{P_{Fan}}{445}\right)^{0.67}$
Heat exchanger [surface area, A_{HE} (m^2); operating pressure, p_{HE} (bar)] [50]	$C_{HE} = 2,\ 546.9 \cdot A_{HE}^{0.67} \cdot p_{HE}^{0.28}$ [€]

sorbent make-up was shown to have a significant impact on the net efficiency in all considered cases. On increasing the relative sorbent make-up from 3% to 7%, the net efficiency was reduced by 2.1% points in the Xe case, 2.2% points in the He and N_2 cases, and 2.3–2.4% points in the remaining cases. The impact of the O_2 content in the flue gas on the thermodynamic performance was shown to be significantly smaller. An increase of this parameter from 1% to 3% caused a marginal decrease in the net efficiency of the single cycle cases (Xe case by 0.16% point; sCO_2 PE2 case by 0.25% points; sCO_2 RC2E2 case by 0.34% points) and the combined cycles cases (He case by 0.62% points; sCO_2 RC2E2/RC2E case by 0.71% points; N_2 case by 0.74% points). A higher reduction in the latter cases was caused by a higher discharge temperature of the clean gas stream that led to a higher outlet loss.

Similarly to the thermodynamic performance, the variation in the relative sorbent make-up rate was shown to have the highest impact on the BEP_{el} in all considered cases. An increase of the relative sorbent make-up from 3% to 7% resulted in an increase in the BEP_{el} by 15.3 €/$MW_{el,net}$h in the sCO_2 RC2E2 and sCO_2 PE2 cases, 20.4 €/$MW_{el,net}$h in the N_2 case, and 17.2–18.9 €/$MW_{el,net}$h in the other cases. The impact of the O_2 content in the flue gas on the economic performance was negligible for single cycle cases, resulting in an increase in BEP_{el} of 0.5–0.8 €/$MW_{el,net}$h. Conversely, its impact on the economic performance of the combined cycle cases was more pronounced, as an increase in the BEP_{el} of 1.7–2.2 €/$MW_{el,net}$h was observed.

4.1.2. Topping cycle parameters

The techno-economic performance of any power generation system is highly influenced by the operating conditions of the power cycle [57], with the highest impact associated with the temperature at the expander inlet and pressure at the outlet of the compressor/pump. Therefore, these parameters, along with three temperature differences, were considered in the parametric study. The maximum live and reheated temperatures of the working medium in all cases were selected based on the minimal temperature difference of 10 °C at the cold end of the FGC. The assumptions for the parametric study are summarised in Table 6.

The effect of the live and reheated temperature of the working medium and main compressor/pump outlet pressure in the single cycle

Table 5
Techno-economic results for coal-fired power plants based on calcium looping combustion under initial assumptions.

Parameter	Case					
	sCO_2 RC2E2	Xe	sCO_2 PE2	He	N_2	sCO_2 RC2E2/RC2E
Thermodynamic assessment						
CCT power requirement (MW_{el})	44.99	44.99	44.99	44.99	44.99	44.99
CaLC power requirement (MW_{el})	18.89	18.89	18.89	18.89	18.89	18.89
sCO_2 cycle power requirement (MW_{el})	7.63	77.77	7.25	7.26	6.91	6.61
Total auxiliary power requirement (MW_{el})	71.51	141.65	71.13	71.14	70.79	70.49
Topping cycle gross power output ($MW_{el,gross}$)	584.05	598.20	581.49	471.09	450.71	501.65
Bottoming cycle gross power output ($MW_{el,gross}$)	–	–	–	33.09	27.72	35.29
Net power output ($MW_{el,net}$)	507.91	456.55	510.36	433.03	407.64	466.45
Net efficiency (%)	34.97	31.43	35.14	29.81	28.06	32.11
Indirect heat transfer efficiency (%)	67.52	67.52	67.52	67.52	67.52	67.52
Specific CO_2 emissions (kg/$MW_{el,net}$h)	101.98	113.37	101.42	119.53	126.97	111.05
Economic assessment						
CCT investment cost (M€)	22.6	22.6	22.6	22.6	22.6	22.61
CaLC investment cost (M€)	395.8	394.1	392.1	384.4	377.7	380.3
Power cycle investment cost (M€)	150.1	106.7*	121.0	170.4	172.9	144.1
Total as-spent investment cost (M€)	1417.0	1322.4*	1348.3	1435.6	1426.7	1372.0
Specific total as-spent investment cost (€/$kW_{el,net}$)	2789.8	2896.5*	2641.9	3315.3	3500.0	2941.3
Break-even price of electricity (€/$MW_{el,net}$h)	78.35	84.52*	76.22	92.23	97.62	83.95

*The cost of filling the cycle with xenon is not taken into consideration.

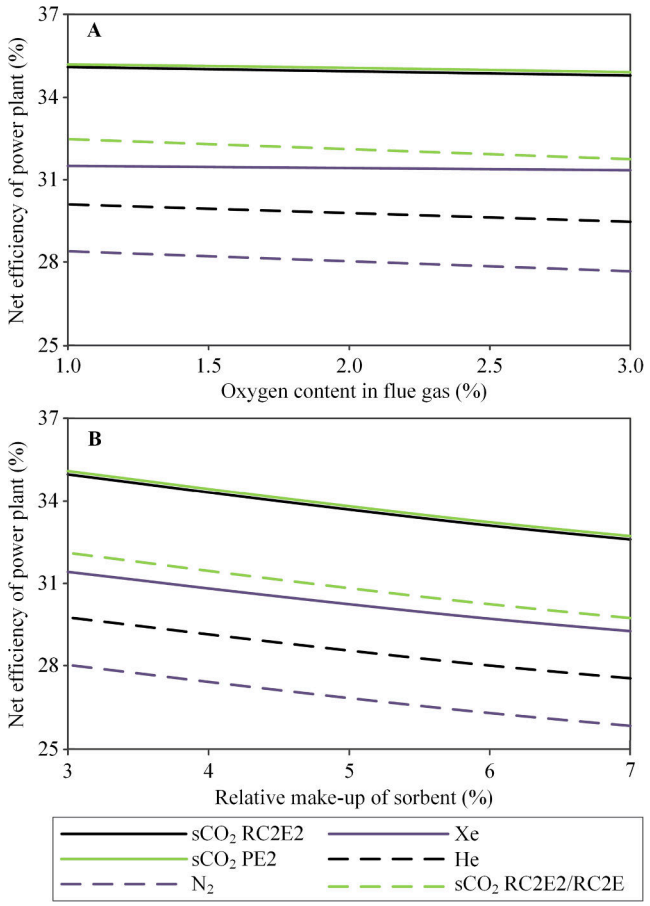


Fig. 5. Effect of (A) oxygen content in flue gas and (B) relative make-up of sorbent on thermodynamic performance.

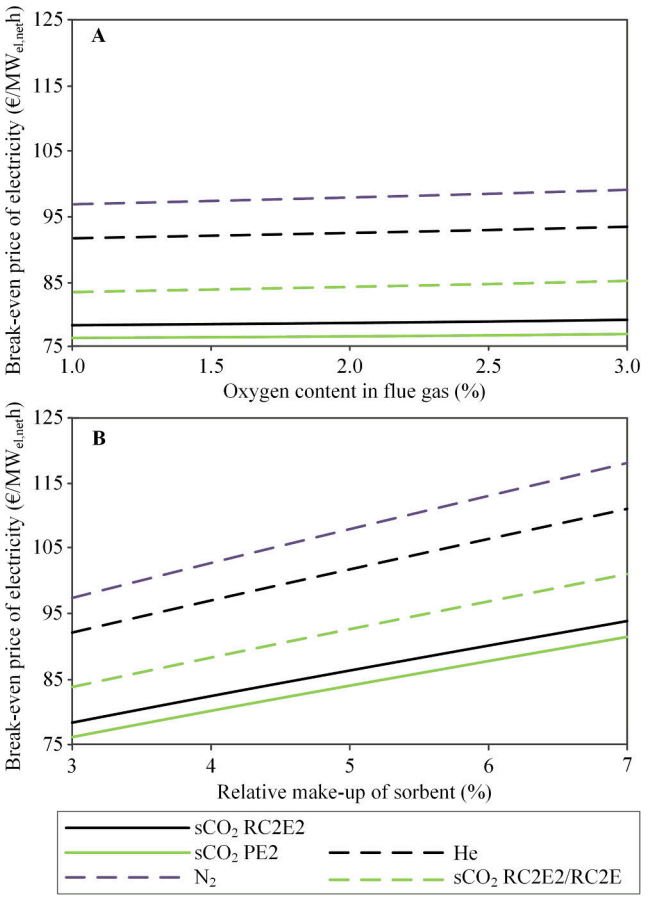


Fig. 6. Effect of (A) oxygen content in flue gas and (B) relative make-up of sorbent on economic performance.

cases (sCO_2 RC2E2, Xe and sCO_2 PE2) on the thermodynamic and economic performance are presented in Fig. 7. The thermodynamic results for the lowest temperature (500 ˚C) indicate that there was an optimal pressure at the outlet of the SCP for both sCO_2 PE2 case (30 MPa) and Xe case (28 MPa). At the highest live and reheated CO_2 temperature, the optimal pressure of 32 MPa was observed for both cases. The economic results for the sCO_2 PE2 case indicate the same optimal pressure for a temperature of 665 ˚C. The techno-economic results for the sCO_2 RC2E2 case revealed that the optimal pressures at both temperatures were higher than the maximal considered value.

The results of the parametric study on the live and reheated temperature of the working medium, as well as the main compressor outlet pressure for the combined cycles cases (He, N_2 and sCO_2 RC2E2/RC2E) are presented in Fig. 8. The techno-economic results for the He case at both presented temperatures revealed that the optimal main compressor outlet pressure was below considered pressure ranges, but the economic results show that the minimal considered pressure of 7 MPa was very close to optimal pressure. In the N_2 case, both net efficiency and the BEP_{el} at the lower temperature (500 ˚C) indicated that the optimal compressor pressure was 21 MPa (24.2%; 113.6 €/$MW_{el,net}$h), while the results at higher temperature showed that the optimal pressure was 25 MPa according to economic results. Finally, in the sCO_2 RC2E2/RC2E case, the optimal compressor pressure was above the considered range at both considered temperatures. In all considered cases (Fig. 7 and Fig. 8), increasing of the temperature resulted in a significant increase in the net efficiency and reduction of BEP_{el}. It should be noted, therefore, that the influence of the temperature on the techno-economic performance was much higher than that of the compressor/pump outlet pressure.

The techno-economic result from the parametric study of the temperature difference at the cold end of RHX1 and RHX2, and at the hot end of RHX2 for sCO_2 RC2E2 and sCO_2 RC2E2/RC2E cases are presented in Fig. 9. The increase in the temperature differences resulted in a decrease in the net efficiency and an increase in the BEP_{el} in all considered cases. The increase in the RHX1 cold-end temperature difference was shown to have the lowest impact on the techno-economic

Table 6
Topping cycle parametric study assumptions.

Parameter	Case	Minimum value	Maximum value
Live and reheated temperature of working medium in the topping cycle (˚C)	sCO_2 RC2E2	500	660
	Xe	500	700
	sCO_2 PE2	500	665
	He	500	665
	N_2	500	665
	sCO_2 RC2E2/RC2E	500	660
Pump/compressor outlet pressure (MPa)	sCO_2 RC2E2	18	30
	Xe	28	40
	sCO_2 PE2	28	40
	He	7	11
	N_2	18	30
	sCO_2 RC2E2/RC2E	18	30
RHX1 cold-end temperature difference (K)	All	5	15
RHX2 cold-end temperature difference (K)	sCO_2 RC2E2 and sCO_2 RC2E2/RC2E	5	15
RHX2 hot-end temperature difference (K)	sCO_2 RC2E2 and sCO_2 RC2E2/RC2E	5	15

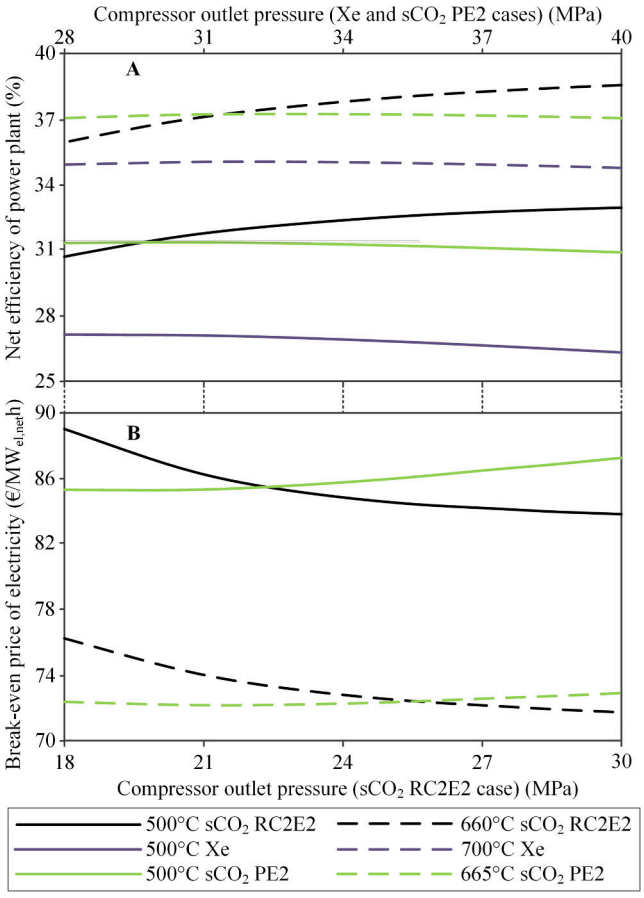


Fig. 7. Effect of live and reheated temperature and the main compressor outlet pressure on (A) thermodynamic and (B) economic performance in the single cycle cases.

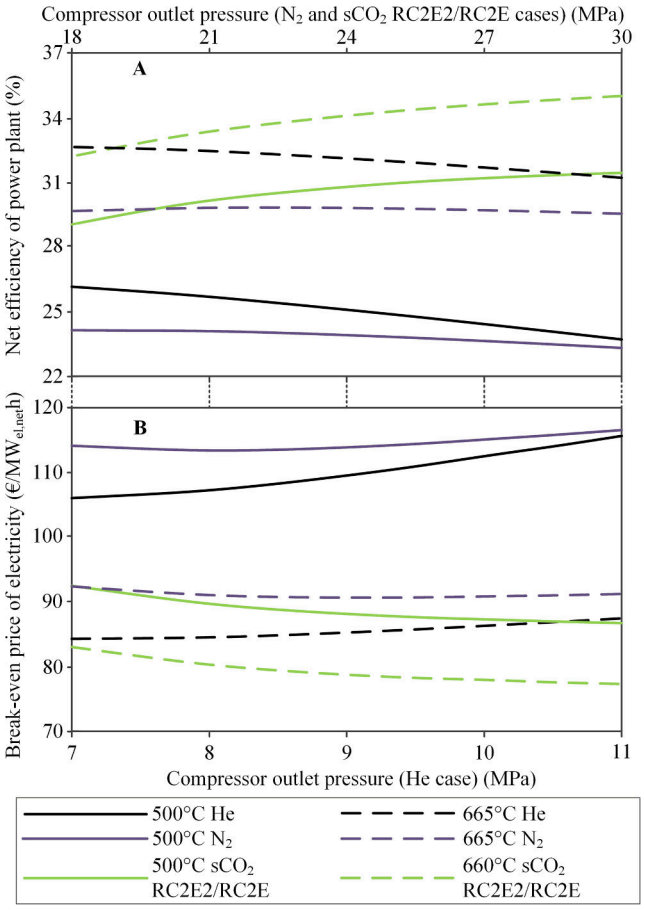


Fig. 8. Effect of live and reheated temperature and the main compressor outlet pressure on (A) thermodynamic and (B) economic performance for combined cycles cases.

performance of the coal-fired power plant based on CaLC. In the sCO_2 RC2E2/RC2E case, the net efficiency decreased by 0.2% point and the BEP_{el} increased by 0.43 €/$MW_{el,net}$h, whereas in the sCO_2 RC2E2 case the net efficiency decreased by 0.3% points and the BEP_{el} increased by 0.38 €/$MW_{el,net}$h. On the other hand, the increase in the RHX2 hot-end temperature difference had the largest effect on the techno-economic performance of the coal-fired power plant based on CaLC, as the net efficiency reduced by 1.4% points and 1.9% points, whereas the BEP_{el} increased by 2.94 €/$MW_{el,net}$h and 3.32 €/$MW_{el,net}$h, in the sCO_2 RC2E2/RC2E and sCO_2 RC2E2 cases, respectively.

The results of the parametric study on the temperature difference at the cold end of RHX1 for Xe, sCO_2 PE2, He and N_2 cases are presented in Fig. 10. The increase in the temperature difference was shown to result in a decrease in the net efficiency in all considered cases. The net efficiency drop was the highest in the N_2 case (1.66% points) and the lowest in the Xe case (0.68% points). For the sCO_2 PE2 and N_2 cases, the BEP_{el} increased with an increase in the temperature difference. For the He case, the BEP_{el} was minimised at the temperature difference of 7.5 °C. Below this value, the increased heat exchanger costs have higher impact on economic results than the increase of the power plant efficiency. This was the opposite in the remaining two cases because of the much higher RHX overall heat transfer coefficient.

4.1.3. Bottoming cycle parameters

To assess the influence of the operating conditions of the bottoming power cycle, a parametric study for the He, N_2 and sCO_2 RC2E2/RC2E cases was performed. The compressor outlet pressure was varied between 11 and 15 MPa for the He case and 18–30 MPa for the N_2 and sCO_2 RC2E2/RC2E cases. The temperature difference was varied in the range of 5–15 °C in all considered cases. In addition, the O_2 content in flue gas of 1% and the revised parameters for the topping cycle (Table 6) were assumed.

The results of the parametric study on the compressor outlet pressure in the bottoming cycle cases are presented in Fig. 11. It has been observed that an increase in the pressure in both the N_2 and sCO_2 cases resulted in an increase in the net efficiency and a reduction in the BEP_{el}. Importantly, the optimal pressure in both cases was above the considered range (> 30 MPa). In the He case, on the contrary, the optimal pressure at the compressor outlet was shown to be 13 MPa and 12 MPa, respectively, considering thermodynamic and economic standpoints.

On variation of the temperature difference at the cold end of the RHX1 between 5 and 15 °C, a negligible change in the net efficiency (< 0.006% points) was observed for all cases. Similarly, the BEP_{el} was shown to decrease marginally by 0.31 €/$MW_{el,net}$h in the He case, 0.27 €/$MW_{el,net}$h in the N_2 case, and 0.02 €/$MW_{el,net}$h in the sCO_2 RC2E2/RC2E case on an increase in the temperature difference. The increase of the RHX2 hot-end temperature difference in the sCO_2 RC2E2/RC2E case resulted in an increase of the net efficiency by 0.04% points and decrease of the BEP_{el} by 0.2 €/$MW_{el,net}$h. In the same case, the increase of the RHX2 cold-end temperature difference caused a decrease of the net efficiency by 0.14% points and increase of the BEP_{el} by 0.2 €/$MW_{el,net}$h. Thus, the impact of the considered temperature differences on the techno-economic performance of the considered cases was found to be small.

4.2. Techno-economic performance under revised parameters

Considering the outcomes of the parametric study, the techno-economic performance of the considered cases was re-assessed. The O_2

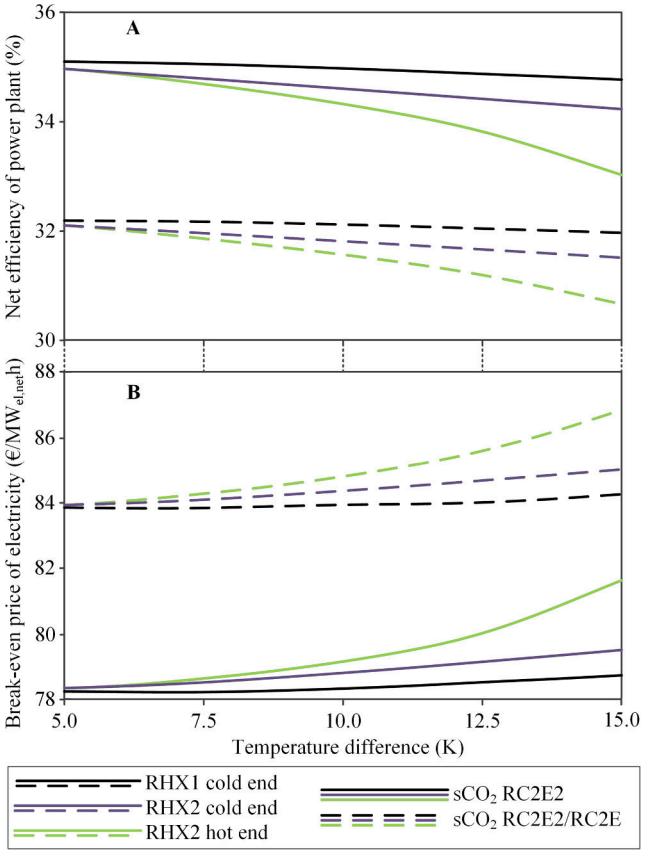


Fig. 9. Effect of the temperature differences of heat recuperation system on (A) thermodynamic and (B) economic performance of sCO_2 RC2E2 and sCO_2 RC2E2/RC2E cases.

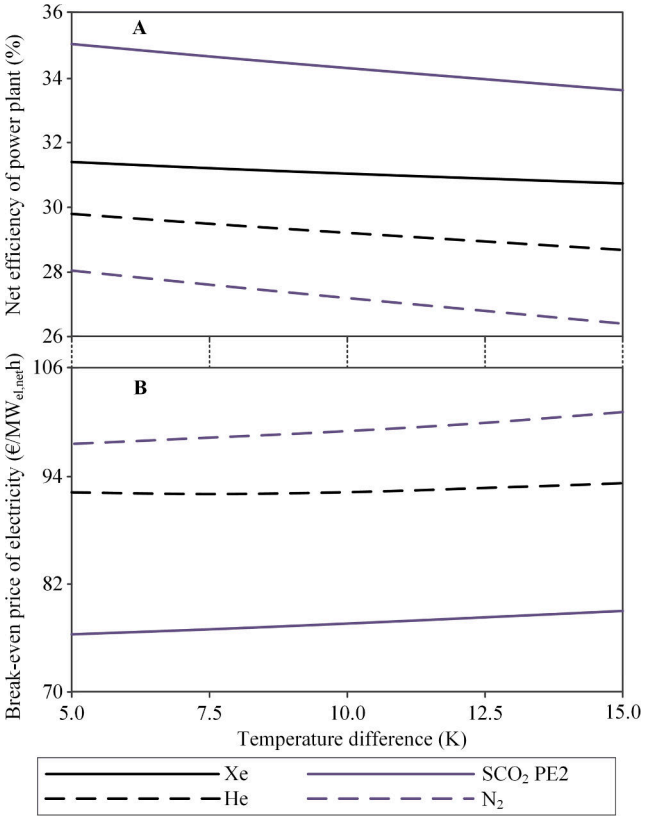


Fig. 10. Effect of the temperature differences on cold side of recuperator on (A) thermodynamic and (B) economic performance for Xe, sCO_2 PE2, He and N_2 cases.

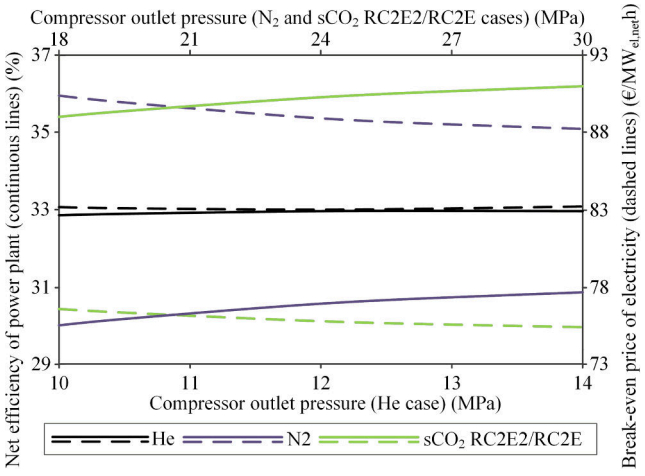


Fig. 11. Effect of the compressor outlet pressure in the bottoming cycle on the techno-economic performance for combined cycle cases.

content in flue gas of 1% for all cases was assumed. The remaining revised parameters, along with thermodynamic and economic results, are presented in Table 7.

As a result of revising the operating conditions in the considered cases of the coal-fired power plant based on CaLC, a significant improvement in the net efficiency was observed. The net efficiency of the sCO_2 RC2E2, Xe and sCO_2 RC2E2/RC2E cases was increased by 4.0–4.1% points. In the remaining cases, improvements of 2.3–3.1% points were achieved. A subsequent improvement in the economic performance was achieved, as the BEP_{el} decreased by 9.5–9.6 €/$MW_{el,net}$h in the Xe, He and N_2 cases, 4.5 €/$MW_{el,net}$h in the sCO_2 PE2 case, and 7.2–8.7 €/$MW_{el,net}$h for the remaining two cases. Importantly, the best techno-economic performance was reported for sCO_2 RC2E2 case, as it achieved a net efficiency of 38.94% and a BEP_{el} of 71.15 €/$MW_{el,net}$h.

Finally, the results revealed that the net efficiency in the sCO_2 RC2E2 case is higher by 0.9% points (38.9%) than that for a conventional coal-fired power plant without CCS (38%) analysed in Hanak and Manovic [19] and Michalski et al. [25]. Nevertheless, the BEP_{el} for the coal-fired power plant based on CaLC and the sCO_2 RC2E2 cycle was 19.3% higher than that of the conventional coal-fired power plant. Nevertheless, such an increase was shown to be less than a third of that for amine scrubbing retrofit (62%) and half that for CaL retrofit (44%) [25]. Therefore, this study has demonstrated that the coal-fired power plant based on CaLC and the advanced power cycles can significantly reduce the economic and energy penalties associated with CCS.

4.3. Alternative bottoming cycles in sCO_2 RC2E2/RC2E case

The BEP_{el} for the sCO_2 combined cycle (RC2E2/RC2E) case was higher by only 4 €/$MW_{el,net}$h than that in the best case (sCO_2 RC2E2). Therefore, an additional analysis has been performed to identify potential improvements in the techno-economic performance of the sCO_2 RC2E2/RC2E case by changing the bottoming cycle. In this analysis, the techno-economic results for sCO_2 RC2E2/RC2E case (thermodynamic results for CaLC, CCT, main sCO_2 cycle and equipment cost of main sCO_2 cycle) and for sCO_2 RC2E2 case (equipment cost of CaLC and CCT, and BEP_{el} of 71.15 €/$MW_{el,net}$h) were used. The specific cost of the bottoming cycle was varied in the range of 100–1100 €/$kW_{el,gross}$ [58]. Based on those assumptions the efficiency of the bottoming cycle for which the NPV is equal to zero was calculated. The results of such analysis are presented in Fig. 12. The required minimal efficiency

Table 7
Techno-economic results for coal-fired power plants based on calcium looping combustion under revised parameters.

Parameter	Case					
	sCO_2 RC2E2	Xe	sCO_2 PE2	He	N_2	sCO_2 RC2E2/RC2E
Assumptions						
Fluid live/reheated temperature (°C)	665	710	670	665	665	665
Topping cycle compressor/pump outlet pressure (MPa)	30	32	32	7	25	30
Bottoming cycle compressor outlet pressure (MPa)	–	–	–	12	30	30
Temperature difference at RHX1 cold end (°C)	5	5.0	5.0	7.5	5	7.5
Temperature difference at RHX2 cold/hot end (°C)	5/5	-/-	-/-	15/-	15/-	5/5
Temperature difference at RHX3 cold end (°C)	–	–	–	–	–	15
Temperature difference at RHX4 cold/hot end (°C)	-/-	-/-	-/-	-/-	-/-	5/15
Thermodynamic assessment						
CCT power requirement (MW)	44.98	44.99	44.99	44.99	44.99	44.98
CaLC power requirement (MW)	18.29	18.29	18.29	18.29	18.29	18.29
sCO_2 cycle power requirement (MW)	6.95	70.34	6.86	6.85	6.84	6.12
Total auxiliary power requirement (MW)	70.22	133.62	70.15	70.14	70.12	69.39
Topping cycle gross power output ($MW_{el,net}$)	640.58	649.00	614.02	500.99	480.17	550.23
Bottoming cycle gross power output ($MW_{el,net}$)	–	–	–	47.71	38.10	45.22
Net power output (MW)	565.64	515.38	543.88	478.56	448.15	526.05
Net efficiency (%)	38.94	35.48	37.44	32.95	30.85	36.22
Specific CO_2 emission ($kg/MW_{el,net}h$)	91.53	100.50	95.24	108.23	115.58	98.41
Economic assessment						
CCT investment cost (M€)	22.6	–	22.6	22.6	22.6	22.6
CaLC investment cost (M€)	395.6	–	392.2	381.6	377.2	379.7
Power cycle investment cost (M€)	164.7	–	123.6	158.7	159.5	157.5
Total as-spent investment cost (M€)	1447.1	–	1353.8	1405.4	1397.6	1398.9
Specific total as-spent investment cost (€/$kW_{el,net}$)	2558.3	–	2489.2	2936.6	3118.6	2659.2
Break-even price of electricity (€/$MW_{el,net}h$)	71.15	–	71.74	82.79	88.07	75.22

increased from 35.2% to 59.6% with an increase of the specific cost. The smallest value corresponds to 65.5% of the Carnot efficiency (53.7%). The specific equipment cost of sCO_2 bottoming cycles considered in this paper were 227.1–368.6 €/$kW_{el,gross}$, which correlate to the cycle efficiency of 37.0–39.3%. The analysed sCO_2 bottoming cycles have higher efficiencies than needed (42.8%), but cannot reduce the temperature of the clean gas to the desired values (85–125 °C) [37]. Therefore, the power output of such bottoming cycles is not sufficient to improve the techno-economic performance over the sCO_2 RC2E2 case. The bottoming cycles based on the conventional steam cycle and Kalina cycle can significantly reduce the temperature of the clean gas, maximising the amount of heat that is utilised for power generation in the bottoming cycle. For the specific equipment cost for high-efficiency steam bottoming cycles of 642 €/$kW_{el,gross}$ [58], the corresponding cycle efficiency is 45.2%. This efficiency is significantly higher than advanced triple-pressure steam bottoming cycle efficiencies (35.7%) reported for higher temperatures of the heat source [59]. The whole cycle efficiency range is also significantly above the cycle efficiencies of Kalina cycles (27.8–30.7%) at the heat source temperatures of 430 °C (27.8%) [60] and 550 °C (30.7%) [61].

4.4. Carbon tax

The results presented above assumed that the carbon tax was zero. Therefore, to understand the influence of the carbon tax on the economic feasibility of the considered cases, the parametric study of the carbon tax was conducted over the range of 0–100 €/t_{CO2}. The results for revised assumptions (Table 7) are presented in Fig. 13.

This study has revealed that the lowest impact of the carbon tax on the economic performance was observed in the sCO_2 RC2E2 case, as the BEP_{el} increased only by 9.2 €/$MW_{el,net}h$. This can be associated primarily with the lowest specific CO_2 emissions among the considered cases. In the remaining cases, the impact on economic effectiveness was slightly higher, as the BEP_{el} increased by 9.5–11.6 €/$MW_{el,net}h$. To benchmark the economic performance of the considered cases, the parametric study of the carbon tax was also performed for the conventional coal-fired power plant without CO_2 capture [25]. It has been shown that on an increase in the carbon tax from 0 to 100 €/t_{CO2}, the BEP_{el} for the conventional coal-fired power plant without CO_2 capture has increased from 59.63 €/$MW_{el,net}h$ to 139.31 €/$MW_{el,net}h$. Importantly, if the carbon tax was above 41.7 €/tCO_2, the economic performance of all the CaLC cases considered in this study was superior to that of the conventional coal-fired power plant without CO_2 capture. Moreover, the cost of CO_2 avoided for the sCO_2 RC2E2 case (16.3 €/t_{CO2}) and the sCO_2 PE2 case (17.3 €/t_{CO2}) was shown to be lower than the carbon tax reported in January and February 2019 (18.35–24.60 €/t_{CO2}) [62]. Therefore, this study has confirmed that commercial deployment of the coal-fired power plant based on CaLC and advanced power cycles can be economically viable under current market conditions.

5. Conclusions

This study aimed to improve the techno-economic performance of coal-fired power plants based on calcium looping combustion by using

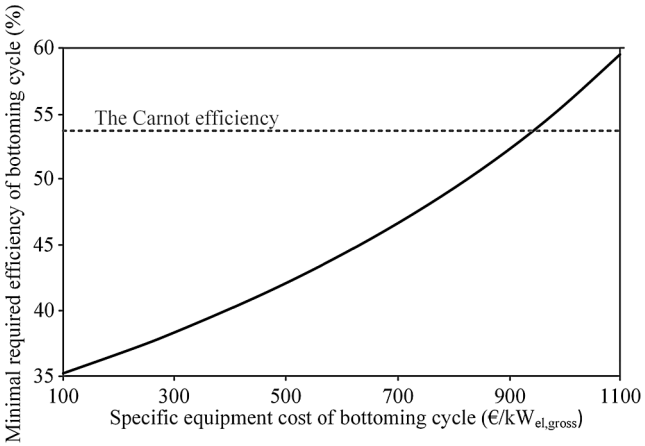


Fig. 12. Identification of the minimum efficiency of the bottoming cycle as a function of the specific equipment cost of bottoming cycle.

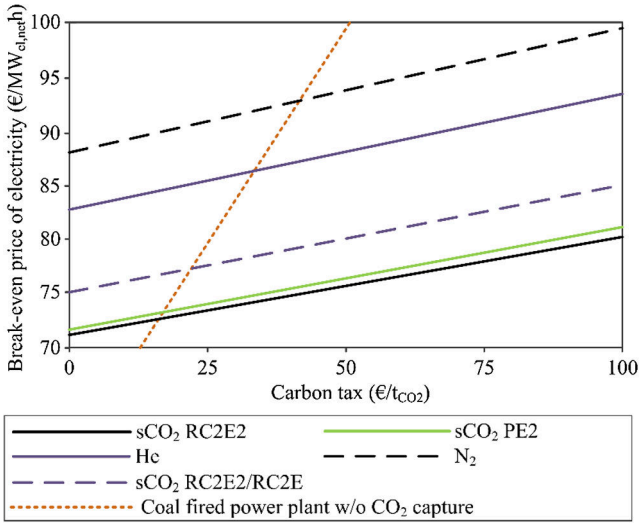


Fig. 13. Effect of carbon tax on the economic performance of coal-fired power plants based on calcium looping combustion.

different structures of, and working media in, advanced power cycles. All considered cases were equipped with the same calcium looping combustion and CO_2 compression train. The net efficiency and the break-even electricity price, which was estimated using the net present value approach, were used as the main techno-economic performance indicators. The parametric study of the considered cases revealed that the live temperature and pump/compressor outlet pressure in the advanced power cycles had the largest impact on the techno-economic performance of the coal-fired power plant based on calcium looping combustion. The results have shown that the recompression supercritical CO_2 cycle (sCO_2 RC2E2 case) had the highest net efficiency (38.9%) and the lowest break-even electricity price (71.15 €/$MW_{el,net}$h) among all considered cases. It needs to be highlighted that the net efficiency of that case was shown to be higher than that of the conventional coal-fired power plant without CO_2 capture (38.0%). Nevertheless, the break-even electricity price for the best case presented in this study was shown to be still 19.3% higher than that for the conventional coal-fired power plant without CO_2 capture (59.63 €/$MW_{el,net}$h). Such an increase was shown to be less than a third of that for amine scrubbing retrofit (62%) and half that for a calcium looping retrofit (44%). Moreover, the corresponding cost of CO_2 avoided was estimated to be 16.3 €/t_{CO2}. As this figure is lower than the current value of the carbon tax (18.35–24.60 €/t_{CO2}), the coal-fired power plant based on calcium looping combustion has been shown to be economically viable under current market conditions.

CRediT authorship contribution statement

Sebastian Michalski: Conceptualization, Methodology, Formal analysis, Visualization, Writing - original draft. **Dawid P. Hanak:** Conceptualization, Validation, Resources, Data curation, Writing - review & editing, Supervision, Funding acquisition. **Vasilije Manovic:** Writing - review & editing, Supervision, Funding acquisition.

Declaration of Competing Interest

The authors declare that they have no known competing financial interests or personal relationships that could have appeared to influence the work reported in this paper.

Acknowledgements

This publication is based on research conducted within the "Redefining power generation from carbonaceous fuels with carbonate looping combustion and gasification technologies" project funded by UK Engineering and Physical Sciences Research Council (EPSRC reference: EP/P034594/1). Data underlying this study can be accessed through the Cranfield University repository at https://doi.org/10.17862/cranfield.rd.12173625.

Appendix A. Supplementary material

Supplementary data to this article can be found online at https://doi.org/10.1016/j.apenergy.2020.114954.

References

[1] UN. Adoption of the Paris Agreement. Paris, France: United Nations Framework Convection on Climate Change; 2015.
[2] IEA. Climate Change and Enviroment 2016 Insights. Paris, France: IEA Publications; 2016.
[3] IEA. 20 years of carbon capture and storage. Accelerating future deployment. Paris, France: IEA Publications; 2016.
[4] Boot-Handford ME, Abanades JC, Anthony EJ, Blunt MJ, Brandani S, Mac Dowell N, et al. Carbon capture and storage update. Energy Environ Sci 2014;7:130–89. https://doi.org/10.1039/C3EE42350F.
[5] Kvamsdal HM, Romano MC, van der Ham L, Bonalumi D, van Os P, Goetheer E. Energetic evaluation of a power plant integrated with a piperazine-based CO_2 capture process. Int J Greenh Gas Control 2014;28:343–55. https://doi.org/10.1016/j.ijggc.2014.07.004.
[6] Renner M. Carbon prices and CCS investment: A comparative study between the European Union and China. Energy Policy 2014;75:327–40. https://doi.org/10.1016/j.enpol.2014.09.026.
[7] Hanak DP, Manovic V. Calcium looping with supercritical CO_2 cycle for decarbonisation of coal-fired power plant. Energy 2016;102:343–53. https://doi.org/10.1016/j.energy.2016.02.079.
[8] Hanak DP, Biliyok C, Anthony EJ, Manovic V. Modelling and comparison of calcium looping and chemical solvent scrubbing retrofits for CO_2 capture from coal-fired power plant. Int J Greenh Gas Control 2015;42:226–36. https://doi.org/10.1016/j.ijggc.2015.08.003.
[9] Hanak DP, Michalski S, Manovic V. From post-combustion carbon capture to sorption-enhanced hydrogen production: A state-of-the-art review of carbonate looping process feasibility. Energy Convers Manage 2018;177:428–52. https://doi.org/10.1016/j.enconman.2018.09.058.
[10] Rossi RA. Indirect heat transfer in fluidised bed dryers and calciners. J Powder Bulk Solids Technol 1984;8:18–24.
[11] Malhotra K, Mujumdar AS. Indirect heat transfer and drying in mechanically agitated granular beds-an annotated bibliography. Dry Technol 1989;7:153–71. https://doi.org/10.1080/07373938908916583.
[12] Lutz R. Preparation of phosphoric acid waste gypsum for further processing to make building materials. ZKG Int Ed B 1994;47:6.
[13] Hatzilyberis KS. Design of an indirect heat rotary kiln gasifier. Fuel Process Technol 2011;92:2429–54. https://doi.org/10.1016/j.fuproc.2011.08.004.
[14] Sánchez Jiménez PE, Perejón A, Benítez Guerrero M, Valverde JM, Ortiz C, Pérez Maqueda LA. High-performance and low-cost macroporous calcium oxide based materials for thermochemical energy storage in concentrated solar power plants. Appl Energy 2019;235:543–52. https://doi.org/10.1016/j.apenergy.2018.10.131.
[15] Chacartegui R, Alovisio A, Ortiz C, Valverde JM, Verda V, Becerra JA. Thermochemical energy storage of concentrated solar power by integration of the calcium looping process and a CO_2 power cycle. Appl Energy 2016;173:589–605. https://doi.org/10.1016/j.apenergy.2016.04.053.
[16] Abanades JC, Anthony EJ, Wang J, Oakey JE. Fluidized bed combustion systems integrating CO_2 capture with CaO. Environ Sci Technol 2005;39:2861–6. https://doi.org/10.1021/es0496221.
[17] Junk M, Reitz M, Strohle J, Epple B. Technical and economical assessment of the indirectly heated carbonate looping process. J Energy Resour Technol 2016;138:042210https://doi.org/10.1115/1.4033142.
[18] Hoeftberger D, Karl J. Self-fluidization in an indirectly heated calciner. Chem Eng Technol 2013;36:1533–8. https://doi.org/10.1002/ceat.201300111.
[19] Hanak DP, Manovic V. Calcium looping combustion for high-efficiency low-emission power generation. J Clean Prod 2017;161:245–55. https://doi.org/10.1016/j.jclepro.2017.05.080.
[20] Marchionni M, Bianchi G, Tsamos KM, Tassou SA. Techno-economic comparison of different cycle architectures for high temperature waste heat to power conversion systems using CO_2 in supercritical phase. Energy Procedia 2017;123:305–12. https://doi.org/10.1016/j.egypro.2017.07.253.
[21] Linares JI, Montes MJ, Cantizano A, Sánchez C. A novel supercritical CO_2 recompression Brayton power cycle for power tower concentrating solar plants. Appl Energy 2020;263:114644https://doi.org/10.1016/j.apenergy.2020.114644.
[22] Zhao Y, Zhao L, Wang B, Zhang S, Chi J, Xiao Y. Thermodynamic analysis of a novel dual expansion coal-fueled direct-fired supercritical carbon dioxide power cycle. Appl Energy 2018;217:480–95. https://doi.org/10.1016/j.apenergy.2018.02.088.
[23] Thanganadar D, Asfand F, Patchigolla K. Thermal performance and economic analysis of supercritical carbon dioxide cycles in combined cycle power plant. Appl

Energy 2019;255:113836https://doi.org/10.1016/j.apenergy.2019.113836.
[24] Khallaghi N, Hanak DP, Manovic V. Gas-fired chemical looping combustion with supercritical CO_2 cycle. Appl Energy 2019;249:237–44. https://doi.org/10.1016/j.apenergy.2019.04.096.
[25] Michalski S, Hanak DP, Manovic V. Techno-economic feasibility assessment of calcium looping combustion using commercial technology appraisal tools. J Clean Prod 2019;219:540–51. https://doi.org/10.1016/j.jclepro.2019.02.049.
[26] Olumayegun O, Wang M, Kelsall G. Thermodynamic analysis and preliminary design of closed Brayton cycle using nitrogen as working fluid and coupled to small modular Sodium-cooled fast reactor (SM-SFR). Appl Energy 2017;191:436–53. https://doi.org/10.1016/j.apenergy.2017.01.099.
[27] Alpy N, Cachon L, Haubensack D, Floyd J, Simon N, Gicquel L, Rodriguez G, Saez M, Laffont G. Gas Cycle testing opportunity with ASTRID, the French SFR prototype. In: Proceedings of Supercritical CO2 Power Cycle Symposium. 2011.
[28] Son S, Jeong Y, Cho SK, Lee JI. Development of supercritical CO_2 turbomachinery off-design model using 1D mean-line method and Deep Neural Network. Appl Energy 2020;263:114645https://doi.org/10.1016/j.apenergy.2020.114645.
[29] Pérez-Pichel GD, Linares JI, Herranz LE, Moratilla BY. Potential application of Rankine and He-Brayton cycles to sodium fast reactors. Nucl Eng Des 2011;241:2643–52. https://doi.org/10.1016/j.nucengdes.2011.04.038.
[30] Garcia RF. Efficiency enhancement of combined cycles by suitable working fluids and operating conditions. Appl Therm Eng 2012;42:25–33. https://doi.org/10.1016/j.applthermaleng.2012.02.039.
[31] Sánchez-Biezma A, Paniagua J, Diaz L, Lorenzo M, Alvarez J, Martínez D, et al. Abanades JC. Testing postcombustion CO_2 capture with CaO in a 1.7 MW_t pilot facility. Energy Procedia 2013;37:1–8. https://doi.org/10.1016/j.egypro.2013.05.078.
[32] Rodríguez N, Alonso M, Abanades JC. Average activity of CaO particles in a calcium looping system. Chem Eng J 2010;156:388–94. https://doi.org/10.1016/j.cej.2009.10.055.
[33] Li Z-S, Cai N-S, Croiset E, Zhen-Shan L, Ning-Sheng C. Process analysis of CO_2 capture from flue gas using carbonation/calcination cycles. AIChE J 2008;54:1912–25. https://doi.org/10.1002/aic.11486.
[34] Perejón A, Romeo LM, Lara Y, Lisbona P, Martínez A, Valverde JM. The Calcium-Looping technology for CO_2 capture: On the important roles of energy integration and sorbent behavior. Appl Energy 2016;162:787–807. https://doi.org/10.1016/j.apenergy.2015.10.121.
[35] Le Moullec Y. Conceptual study of a high efficiency coal-fired power plant with CO_2 capture using a supercritical CO_2 Brayton cycle. Energy 2013;49:32–46. https://doi.org/10.1016/j.energy.2012.10.022.
[36] Park JH, Bae SW, Park HS, Cha JE, Kim MH. Transient analysis and validation with experimental data of supercritical CO_2 integral experiment loop by using MARS. Energy 2018;147:1030–43. https://doi.org/10.1016/j.energy.2017.12.092.
[37] Ciukaj S, Pronobis M. Dew point of the flue gas of boilers co-firing biomass with coal. Chem Process Eng 2013;34. https://doi.org/10.2478/cpe-2013-0009.
[38] Miyamoto J, Hasegawa Y, Yawata N, Wajima K, Ueda K. High-efficiency and compact centrifugal chiller. JRAIA International Symposium. Kobe, Japan: JRAIA; 2016.
[39] Coco-Enríquez L, Muñoz-Antón J, Martínez-Val JM. New text comparison between CO_2 and other supercritical working fluids (ethane, Xe, CH_4 and N_2) in line- focusing solar power plants coupled to supercritical Brayton power cycles. Int J Hydrogen Energy 2017;10:17611–31. https://doi.org/10.1016/j.ijhydene.2017.02.071.
[40] Doran PM. Chapter 9 - Heat Transfer. In: Doran PM, editor. Bioprocess Engineering Principles 2nd ed.UK, London: Academic Press; 2013. p. 333–77. https://doi.org/10.1016/B978-0-12-220851-5.00009-5.
[41] Kunitomi K, Katanishi S, Takada S, Takizuka T, Yan X. Japan's future HTR - The GTHTR300. Nucl Eng Des 2004;233:309–27. https://doi.org/10.1016/j.nucengdes.2004.08.026.
[42] Bai Y, Bai Q. Heat transfer and thermal insulation. Subsea Engineering Handbook. Boston, MA, USA: Gulf: Professional Publishing; 2010. p. 401–50. https://doi.org/10.1016/B978-1-85617-689-7.10014-7.
[43] Bai Y, Bai Q. Chapter 19 - Heat transfer and thermal insulation. In: Bai Y, Bai Q, editors. Subsea Pipelines and Risers Oxford: Elsevier Science Ltd; 2005. p. 317–56. https://doi.org/10.1016/B978-008044566-3.50021-X.
[44] Fout T, Zoelle A, Keairns D, Turner M, Woods M, Kuehn N, Shah V, Chou V. Cost and performance baseline for fossil energy plants volume 1a: bituminous coal (PC) and natural gas to electricity. Pittsburgh, PA, USA: National Energy Technology Laboratory; 2015.
[45] Eurostat. Database - Eurostat 2018.
[46] EDF Energy. Cottam and West Burton | Power stations | EDF Energy 2018.
[47] EURACOAL. Market report 2/2017. EURACOAL; 2017.
[48] Benjelloun M, Doulgeris G, Singh R. A method for techno-economic analysis of supercritical carbon dioxide cycles for new generation nuclear power plants. Proc Inst Mech Eng Part A J Power Energy 2012;226:372–83. https://doi.org/10.1177/0957650911429643.
[49] Criado YA, Arias B, Abanades JC. Calcium looping CO_2 capture system for back-up power plants. Energy Environ Sci 2017;10:1994–2004. https://doi.org/10.1039/c7ee01505d.
[50] Gabbrielli R, Singh R. Economic and scenario analyses of new gas turbine combined cycles with no emissions of carbon dioxide. J Eng Gas Turbines Power 2005;127:531. https://doi.org/10.1115/1.1850492.
[51] Hanak DP, Manovic V. Combined heat and power generation with lime production for direct air capture. Energy Convers Manag 2018;160:455–66. https://doi.org/10.1016/j.enconman.2018.01.037.
[52] Shirazi A, Aminyavari M, Najafi B, Rinaldi F, Razaghi M. Thermal-economic-environmental analysis and multi-objective optimization of an internal-reforming solid oxide fuel cell-gas turbine hybrid system. Int J Hydrogen Energy 2012;37:19111–24. https://doi.org/10.1016/j.ijhydene.2012.09.143.
[53] Lee YD, Ahn KY, Morosuk T, Tsatsaronis G. Exergetic and exergoeconomic evaluation of a solid-oxide fuel-cell-based combined heat and power generation system. Energy Convers Manag 2014;85:154–64. https://doi.org/10.1016/j.enconman.2014.05.066.
[54] Chemicool. Periodic table of elements and chemistry 2018. chemicool.com (accessed April 18, 2019).
[55] BOC. BOC Online Shop 2019. Available at: https://www.boconline.co.uk/shop/en/uk/home.
[56] Hanak DP, Anthony EJ, Manovic V. A review of developments in pilot plant testing and modelling of calcium looping process for CO_2 capture from power generation systems. Energy Environ Sci 2015;8:2199–249. https://doi.org/10.1039/C5EE01228G.
[57] Alfellag MAA. Parametric investigation of a modified gas turbine power plant. Therm Sci Eng Prog 2017;3:141–9. https://doi.org/10.1016/j.tsep.2017.07.004.
[58] Kotowicz J, Brzęczek M, Job M. The thermodynamic and economic characteristics of the modern combined cycle power plant with gas turbine steam cooling. Energy 2018;164:359–76. https://doi.org/10.1016/j.energy.2018.08.076.
[59] Kotowicz J, Job M, Brzeczek M. The characteristics of ultramodern combined cycle power plants. Energy 2015;92:197–211. https://doi.org/10.1016/j.energy.2015.04.006.
[60] Modi A, Knudsen T, Haglind F, Clausen LR. Feasibility of using ammonia-water mixture in high temperature concentrated solar power plants with direct vapour generation. Energy Procedia 2014;115:276–87. https://doi.org/10.1016/j.egypro.2014.10.192.
[61] Modi A, Kærn MR, Andreasen JG, Haglind F. Thermoeconomic optimization of a Kalina cycle for a central receiver concentrating solar power plant. Energy Convers Manag 2016;115:276–87. https://doi.org/10.1016/j.enconman.2016.02.063.
[62] Business Insider. Price of CO_2 European Emission Allowances and Chart. Markets Insider 2019. Available at: https://markets.businessinsider.com/commodities/co2-european-emission-allowances.



https://dspace.org/

Advanced power cycles for coal-fired power plants based on calcium looping combustion: a techno-economic feasibility assessment

Michalski, Sebastian; Hanak, Dawid P.; Manovic, Vasilije

2020-04-27
Elsevier
https://doi.org/10.1016/j.apenergy.2020.114954
Michalski S, Hanak DP, Manovic V. (2020) Advanced power cycles for coal-fired power plants based on calcium looping combustion: a techno-economic feasibility assessment. Applied Energy, Volume 269, July 2020, Article number 114954

Downloaded from a DSpace repository. https://dspace.org/